Scientific Research and Essays Vol. 5(15), pp. 2004-2015, 4 August, 2010
Available online at http://www.academicjournals.org/SRE
ISSN 1992-2248 ©2010 Academic Journals

Full Length Research Paper

Predicting the chloride content from the color analysis for various cement-based materials

Rüstem Gül, Murat Yavuz and Abdulkadir Cüneyt Aydin*

Department of Civil Engineering, Faculty of Engineering, Ataturk University, Erzurum 25240, Turkey.

Accepted 13 July, 2010

The rate of chloride content is of great importance for the performance of reinforced concrete structures exposed to chloride-contaminated environments. The chlorides are known to cause corrosion of metals embedded in cement-based materials. Thus, an important criterion for the evaluation of reinforced concrete structures is the measurement of the chloride content. This is normally done using time consuming standard methods. This paper presents the determination of the apparent chloride content of various cement-based materials using color analysis, which provides the advantages of a fast measurement and the potential for on-site application. The surface can be scanned, or depth profiles are available from cores. Measurements can be performed directly on the sample surface and the results are available in near real time. The results of color analysis method are compared with the results of the Volhard, ion-meter, and Scanner Electron Microscope methods.

Key words: Chloride content, color analysis, electrical resistance, pozzolans, cement-based materials.

INTRODUCTION

Concrete is a multiphase exceedingly complex heterogeneous material and one of the principal materials for structures. However, the heterogeneous structure of concrete, results in some undesirable effects. The heterogeneity and properties of concrete are mostly concerned with the hydration. Hydration, the chemical reaction between water and ingredients of cement is one of the most important properties of its durability and strength gain process. This property of hydration caused a change in the volume of hydrated cement, varying hydration rate through the concrete and time dependency of strength gain and durability. One of the main reasons of durability is the chloride ingress in cement based materials. The durability properties of cement based materials are needed by designers for the proper usage of it in various environments and structural applications. For this reason, determination of chloride diffusion properties of concrete has become very important from the design point of view (Aydın et al., 2010; Hasar et al., 2010; Hasar et al., 2009; Aydın et al., 2008; Gül et al., 2007; Aydın et al., 2007; Aydın, 2007; Aydın and Gül, 2007; Aydın et al., 2006; Düzgün et al., 2005; Tortum et al., 2005; Oğuz and Aydın, 2003).

Durability of reinforced concrete is largely controlled by the capability of the concrete cover to protect the steel reinforcement from corrosion. Despite inherent protective qualities of cement based materials, the corrosion of steel reinforcement has become the most common cause of failure in concrete structures. The service life of a concrete structure, with regard to corrosion of reinforcement in the marine environment, can be considered as, the initiation period, during which the steel remains passive while chloride ions diffuse into the concrete surface; and the propagation (corrosion) period, which begins with depassivation, and during which corrosion propagates at a significant rate up to an acceptable degree of damage. One of the important factors affecting the durability and service life of reinforced concrete structures is the corrosion of embedded steel reinforcing bars. The rate of corrosion in the propagation stage is mainly depends on the electrical resistance of the concrete, its moisture content, oxygen availability, and temperature. The ingress of fluids containing aggressive agents is a necessary condition for many forms of concrete deterioration such as chloride-induced corrosion of reinforcing steel, which can occur either when the material is manufactured or during its subsequent

*Corresponding author. E-mail: acaydin@atauni.edu.tr. Tel: +90 442 231 47 81. Fax: +90 442 236 09 57.

Table 1. Chemical components of PC, FA, SF, and GBFS (%).

Component	PC	FA	SF	GBFS
	(%)			
SiO_2	25.92	54.1	85 - 95	39.56
Fe_2O_3	3.96	9.11	0.5 - 1.0	0.33
Al_2O_3	6.88	21.29	1 - 3	10.82
CaO	53.28	5.93	0.8 - 1.2	37.68
MgO	3.21	6.77	1.0 - 2.0	6.79
SO_3	2.83	0.48	-	0.33
TiO_2	0.20	-	-	-
Sulphide (S^{-2})	0.22	-	-	-
Chloride (Cl^-)	0.017	0.008	-	-
Undetermined	0.49	0.46	-	-
Free CaO	0.35	0.99	-	-
LOI	2.84	0.84	0.5 - 1.0	-

Table 2. Physical and mechanical properties of PC.

	PC
Density (g/cm^3)	3.03
Specific surface (cm^2/g)	3520
Reminder on 200 µm sieve (%)	0.1
Reminder on 90 µm sieve (%)	3.1
Setting time start (min)	132
Setting time end (min)	178
Volume expansion (Le Chatelier, mm)	3
Compressive strengtgh (Mpa)	
2 days	15.6
28 days	38.0

exposure to a chloride-laden environment where it comes into contact with seawater or deicing salt. Because of the highly alkaline environment of cement based systems, a protective passive layer is formed on the metal system. Above certain level of chloride concentrations (chloride threshold value), this protective layer disrupts. The adequacy of that protection is dependent upon the amount of concrete covers, the properties of the concrete, the details of the construction, and the degree of exposure to chlorides from concrete-making components and external sources. The chloride ion ingress is governed by diffusion mechanism and convection. Once a sufficient quantity of chloride has been accumulated on the surface of reinforcement, pitting corrosion will occur. Generally, the diffusion of chloride into concrete is very slow, if the concrete cover does not deteriorate. Because a significant number of structures are exhibiting corrosion of reinforcement, many practitioners and researchers commonly need to determine the chloride concentration in these cement-based materials. The standard methods are time consuming and often expensive and requires larger amounts of cement based materials. A faster, more economical method to determine the chloride concentration of cement-based materials that requires smaller quantities and uses readily available equipment would be beneficial for both research and the industry. A simple and easy method that can be used in field investigations to estimate the depth of penetration of soluble chlorides in concrete was always desirable (Titherington, 1998; Page and Page, 2007; Halmen and Trejo, 2007; Erdoğdu et al., 2004; Nagesh and Bhattacharjee, 1998; ACI 201.2R – 01, 2001; Jin et al., 2007; Meck and Sirivivatnanon, 2003; Güneyisi et al., 2007; Jaegermann, 1990; Song et al., 2008; Topcu et al., 2009).

The reported form of the color analysis method was provided to establish a relations with the chloride content in cement based materials. The determination of the apparent chloride content of various cement-based materials using color analysis provides the advantages of a fast measurement and the potential for on-site application. A rapid method of chloride content analysis produces well correlated results more quickly than the standard time-consuming, and more labor-intensive traditional methods can save significant time and money. The apparent work also deals with mineral admixtures, such as silica fume (SF), fly ash (FA), and granulated blast furnace slag (GBFS) and four water-cement ratios (0.30, 0.4, 0.44, and 0.50).

EXPERIMENTAL DESIGN AND MATERIALS

Portland cement (CEM I 32.5) (PC) from Aşkale, Erzurum in Turkey was used in this study. Maximum aggregate size was 16 mm. The w/c ratios (water-cement ratio) of the mixtures were kept constant at 0.30, 0.40, 0.44, and 0.50 throughout this study. The mineral admixtures; silica fume (SF), granulated blast furnace slag (GBFS), and fly ash (FA - from Tuncbilek, Kütahya, TURKEY) are used (0 and 5%; 0, 35, and 50%; and 0, 20, 25, and 30% by cement weight, respectively). The chemical composition, physical properties of the materials used in this study, some properties of aggregates and concrete mixes are summarized in Tables 1, 2, 3 and 4. The ASTM D 75, ASTM C 136, and ASTM C 29 were used for sampling, grading (Figure 1), unit weight and fineness modulus of aggregates, respectively. A melamine sulphonate polymer based water reducing plasticizing agent is used as superplasticizer (SP) in all mixes. Two series of specimens were prepared for air and water curing. The design of concrete mixtures and some fresh properties are represented in Table 4. At the end of curing regime, the samples are tested at 28th day.

Non-destructive test method (ultrasonic pulse velocity) in the definition of strength properties was considered in this paper. It should be recalled that ultrasonic pulse velocity (UPV) technique is based on the ability to measure the propagation velocity of a pulse of vibration energy, which passes through a concrete medium. In knowing the direct path length between the transducers and the time of travel, the pulse velocity through the concrete can be obtained. Relationship between pulse velocity and strength are determined by calibration tests. UPV measurement techniques are totally non-destructive and advantageous in that they are quick and easy to perform. Also, because of the nature of the test, all the concrete located between the transmitter and the receiver affects the measured property. Therefore, if an experienced operator performs the test, then a considerable amount of useful information can be gained about the interior of a concrete element. UPV was

Table 3. Some properties of aggregates.

Property/effective radius of aggregate	0 - 2 mm	2 - 4 mm	4 - 8 mm	8 - 16 mm
Unit weight (kg/m^3)	1249	1526	1477	1533
Density (kg/m^3)	2200	2485	2535	2598
Water content (%)	3.2	2.49	2.01	0.581
Compacity	0.57	0.61	0.58	0.59
Porosity	0.43	0.39	0.42	0.41
Chloride content (kg/m^3)	0.085	0.076	0.054	0.032
Fine material content	2.4	1.8	1.1	0.2

Table 4. Design of concrete mixtures and fresh properties.

	W	C	FA	SF	GBFS	SP	Aggregate (kg/m^3)			Slump (cm)	UW♦ (kg/m^3)	AC$^{\Psi}$ (%)
	(kg/m^3)						0-2	2-8	8-16			
0M013500♣	116.40	428.57	0.00	0.00	0.00	5.15	548.38	616.93	548.38	3.82	2212	1.23
0M014000	115.53	375.00	0.00	0.00	0.00	2.48	562.46	632.77	562.46	2.91	2216	2.81
0M014400	115.00	340.91	0.00	0.00	0.00	0.00	571.42	642.84	571.42	2.89	2198	2.76
0M015000	114.32	300.00	0.00	0.00	0.00	0.00	582.18	654.94	582.18	4.20	2189	2.98
20M023500	117.15	342.86	85.71	0.00	0.00	5.15	536.07	603.09	536.07	3.45	2187	2.65
20M024000	116.19	300.00	75.00	0.00	0.00	2.48	551.70	620.66	551.70	3.24	2176	3.01
20M024400	115.59	272.73	68.18	0.00	0.00	0.00	561.63	631.84	561.63	3.67	2170	3.26
20M025000	114.85	240.00	60.00	0.00	0.00	0.00	573.57	645.26	573.57	4.02	2169	4.02
30M033500	117.53	300.00	128.57	0.00	0.00	5.15	529.93	596.17	529.93	1.20	2168	2.54
30M034000	116.53	262.50	112.50	0.00	0.00	2.45	546.32	614.61	546.32	2.30	2155	2.43
30M034400	115.88	236.64	102.27	0.00	0.00	0.00	556.75	626.34	556.75	2.80	2150	3.56
30M035000	115.12	210.00	90.00	0.00	0.00	0.00	569.25	640.41	569.25	3.95	2112	4.02
0M543500	118.66	407.14	0.00	21.43	0.00	5.15	511.34	575.26	511.34	4.50	2110	1.23
0M544000	117.53	356.25	0.00	18.75	0.00	2.97	530.05	596.31	530.05	2.89	2104	1.43
0M544400	116.79	323.86	0.00	17.05	0.00	0.00	541.96	609.69	541.96	3.50	2102	2.18
0M545000	115.91	285.00	0.00	15.00	0.00	0.00	556.25	625.78	556.25	4.95	2119	2.13
0M053535	116.54	278.57	0.00	0.00	150.00	5.15	546.03	614.28	546.03	5.15	2219	3.26
0M054035	115.66	243.75	0.00	0.00	131.25	2.45	560.41	630.45	560.41	4.85	2202	2.45
0M054435	115.10	221.59	0.00	0.00	119.32	0.00	569.56	640.75	569.56	3.97	2198	3.46
0M055035	114.43	195.00	0.00	0.00	105.00	0.00	580.53	653.10	580.53	4.37	2183	4.56
0M063550	116.60	214.29	0.00	0.00	214.29	5.15	545.03	613.15	545.03	1.02	2215	1.34
0M064050	115.72	187.50	0.00	0.00	187.50	2.45	559.53	629.47	559.53	0.98	2203	1.01
0M064450	115.15	170.45	0.00	0.00	170.45	0.00	568.75	639.85	568.75	2.34	2181	2.53
0M065050	114.47	150.00	0.00	0.00	150.00	0.00	579.83	652.31	579.83	4.34	2190	3.76
0M573535	118.81	257.14	0.00	21.43	150.00	6.18	509.00	572.62	509.00	1.21	2106	3.46
0M574035	117.65	225.00	0.00	18.75	131.25	2.97	528.00	594.00	528.00	1.01	2103	2.65
0M574435	116.91	204.55	0.00	17.05	119.32	0.00	540.08	607.59	540.08	1.67	2110	3.45
0M575035	116.03	180.00	0.00	15.0	105.00	0.00	554.60	623.93	554.60	2.01	2113	5.62
25M583500	119.62	300.00	107.14	21.43	0.00	6.18	495.96	557.96	495.96	0.85	2056	1.02
25M584000	118.34	262.50	93.75	18.75	0.00	2.97	516.60	581.18	516.60	0.87	2008	0.98
25M584400	117.53	238.64	85.23	17.05	0.00	0.00	529.72	595.94	529.72	1.27	2025	1.12
25M585000	116.57	210.00	75.00	15.00	0.00	0.00	545.49	613.67	545.49	2.01	2016	1.43

♣0M13500: The numbers before M character indicates % content of fly ash, according to cement weight, the first number after M character indicates % content of silica fume, according to cement weight; The last two numbers indicates % content of ground blast furnace slag, according to cement weight; the second number after M character defines the mixture group number, and the two digits after the mixture group number, is the % w/c ratio of the mix. *According to cement weight ♦Fresh unit weight $^{\Psi}$ % air content. W: Water C: Cement SF: Silica fume FA: Flay ash GBFS: Ground blast furnace slag SP: Superplasticizer.

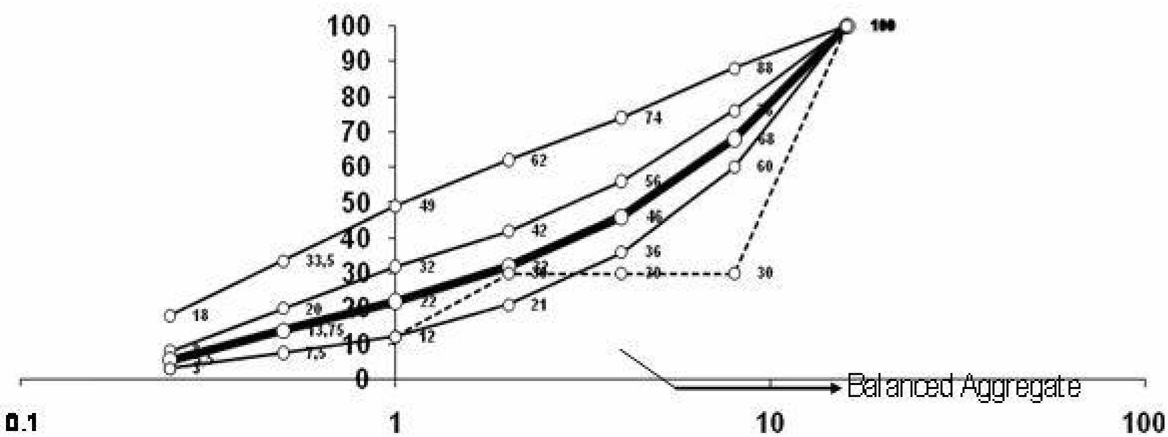

Figure 1. Gradation of aggregate (D_{max} = 16 mm).

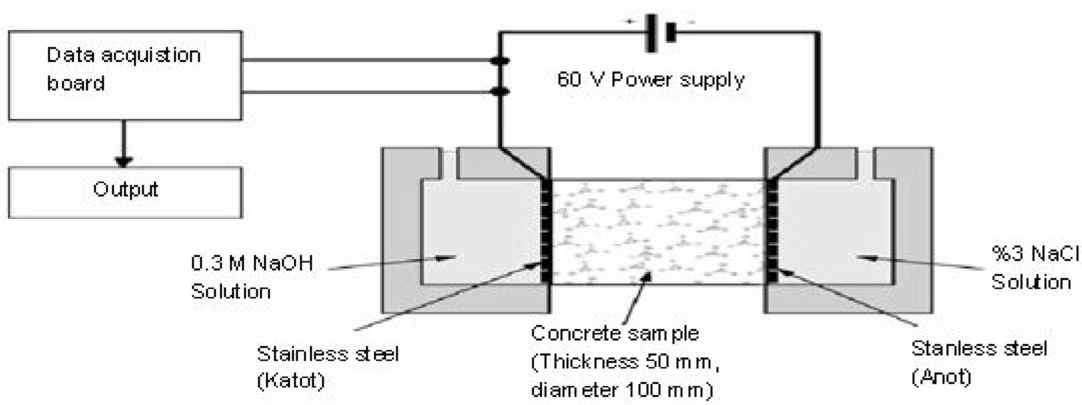

Figure 2. ASTM C1202 test set up.

measured with the portable ultrasonic non-destructive digital indicating tester (Türkmen et al., 2003).

The chloride penetration to hardened concrete specimens is tested electrochemically, according to ASTM C1202. The most controversial point of this method is the voltage and period of voltage application. However, the most widely accepted period and voltage are used according to literature (Samaha and Hover, 1992; Saito and Ishimori, 1995; Goodspeed et al., 1996; RILEM TC 178-TMC, 2002). The specimens are kept in a two cell test room (Figure 2) for six hours at 60 V DC. The current across the specimens is recorded at every 30 min interval by using a computer controlled real-time monitoring system. The total charge passed through the specimens was computed by knowing the current and time history. The presented results are the averages from three specimens.

The chloride content of concrete samples is tested according to Volhard, Ionmeter, Scanner Electron Microscope (SEM), and Color Analysis (CA) Methods. By means of Volhard's method; the chloride content of concrete is determined in the resulting solution of the sample attack with diluted hot nitric acid. The cement based composite sample is treated with diluted HNO_3 and heated to boil in order facilitate the attack and to eliminate sulphides; Cl^- ions in solution are precipitated into AgCl by adding a known excess of a standardized $AgNO_3$ solution. The precipitate is filtered, washed and discarded. The excess of Ag^+ ion is determined in the filtrate by titration with a standardized ammonium thiocyanate solution, using Fe^{3+} solution as a visual indicator. This procedure follows, essentially, those described elsewhere (Basset et al., 1978; Asociacion Espanola de Normalizacion y Certificacion, 1994; Asociacion Espanola de Normalizacion y Certificacion, 1991; Marinus, 2002; Ozyildirim and Halstead, 1988; Chau, 2000; Chau, 2002; Chau, 2004). The ion-selective electrode is essentially the more accurate laboratory version of the well known RCT-method (Rapid Chloride Test) that was developed by Danish Germann-Pedersen. Ion-selective electrodes have been used earlier in determination of chloride in concrete. This test is based on a relationship between the electrical conductance and the resistance to chloride ion penetration (Ozyildirim and Halstead, 1988). SEM is an electron microscope that forms a three-dimensional high resolution image by moving a beam of focused electrons across an object and reading both the electrons scattered by the object and the secondary electrons produced by it. When SEM is used with X-ray diffraction (XRD) techniques, which reveal information about the crystallographic structure, chemical composition and physical properties of materials, the elements and components of concrete sample may be analyzed (Figures 3, 4, and 5). The main principle of CA, is the color change in the pixels of parallel surfaces to concrete sample surfaces, which are exposed to chloride ions. The percentage of the color changing pixels and depth graphs can be used to observe chloride penetration by using predicted empiric formulation (Figures 6 and 7).

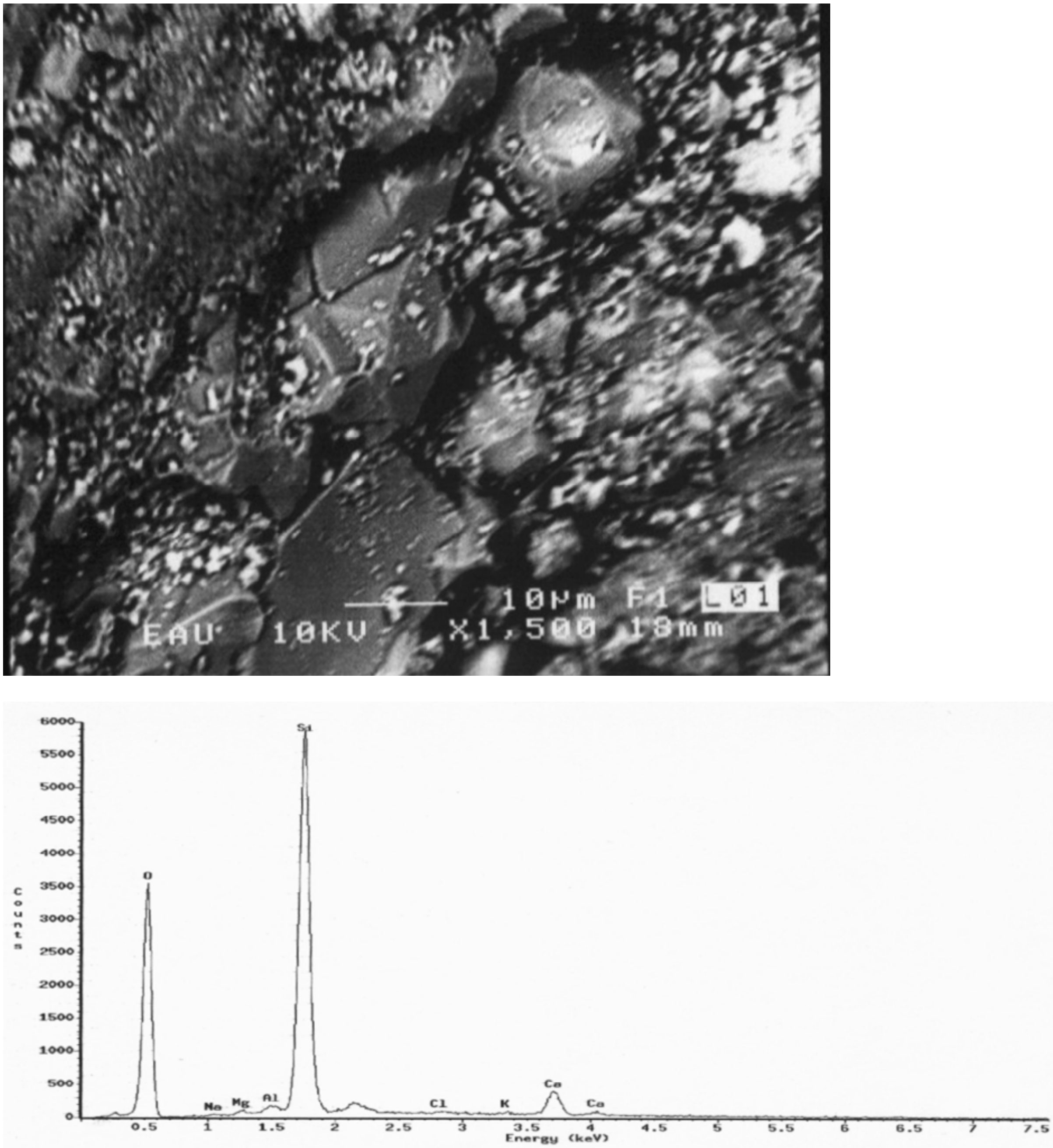

PROZA Correction Acc.Volt.= 10 kV Take-off Angle=32.89 deg
Number of Iterations = 3

Element	k-ratio (calc.)	ZAF	Atom %	Element Wt %	Wt % Err. (1-Sigma)	Compound Formula	Compound Wt %	No. of Cations
Fe-K	0.0200	1.207	1.28	2.42	+/- 1.07	Fe2O3	3.46	16.000
Cl-K	0.0002	1.239	0.02	0.02	+/- 0.12	Cl	0.02	0.238
Ag-L	0.0000	1.445	0.00	0.00	+/- 0.00	Ag2O	0.00	0.000
Si-K	0.7578	1.028	82.35	77.94	+/- 0.43	Si	77.94	1025.641
Al-K	0.0096	1.054	1.11	1.01	+/- 0.08	Al	1.01	13.799
K -K	0.0069	1.139	0.60	0.79	+/- 0.15	K	0.79	7.458
Ca-K	0.1466	1.106	12.00	16.20	+/- 0.50	Ca	16.20	149.410
Mg-K	0.0053	1.099	0.71	0.58	+/- 0.06	Mg	0.58	8.891
O -K	---	2.962	1.93	1.04 S	---	---	---	---
Total			100.00	100.00			100.00	1221.438

Figure 3. SEM and XRD analysis of chloride diffused samples (No white sediment).

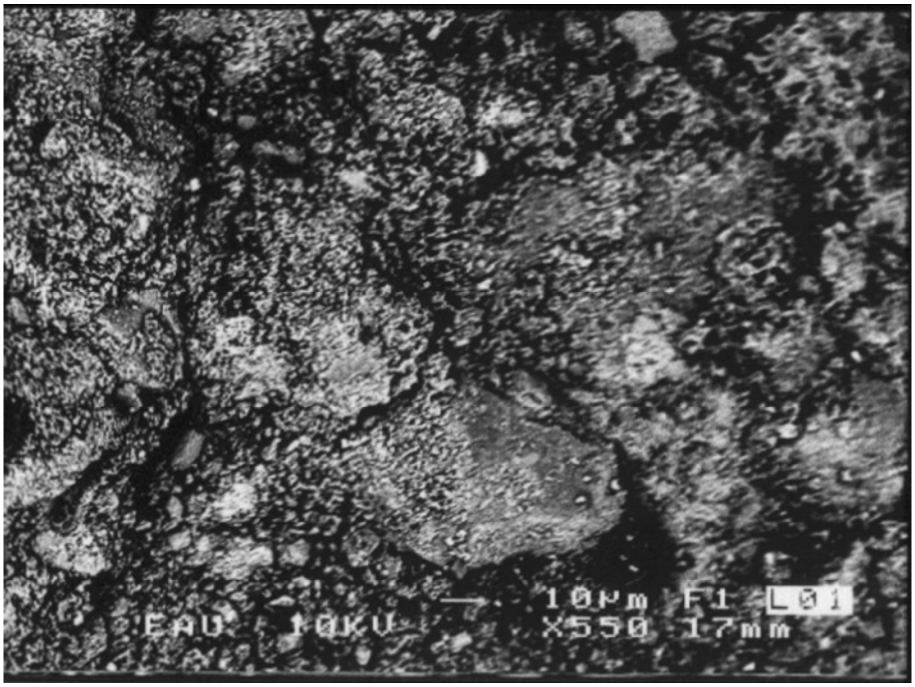

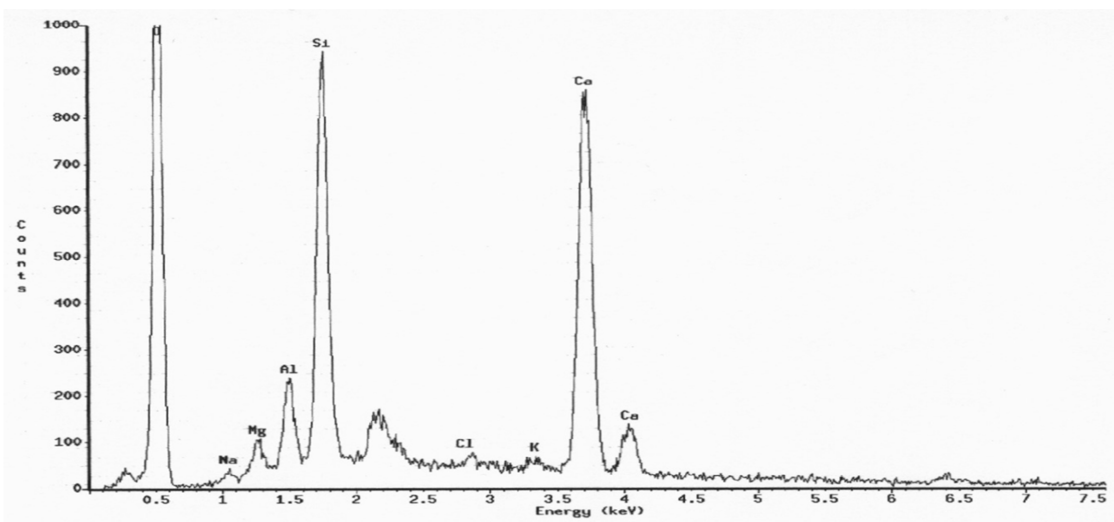

PROZA Correction Acc.Volt.= 10 kV Take-off Angle=31.95 deg
Number of Iterations = 4

Element	k-ratio (calc.)	ZAF	Atom %	Element Wt %	Wt % Err. (1-Sigma)	Compound Formula	Compound Wt %	No. of Cations
Fe-K	0.1016	1.166	7.36	11.84	+/- 2.37	Fe2O3	16.93	16.000
Cl-K	0.0006	1.082	0.07	0.07	+/- 0.23	Cl	0.07	0.142
Ag-L	0.0000	1.268	0.00	0.00	+/- 0.00	Ag2O	0.00	0.000
Si-K	0.1804	1.109	24.71	20.00	+/- 0.51	Si	20.00	53.756
Al-K	0.0307	1.209	4.77	3.71	+/- 0.21	Al	3.71	10.380
K -K	0.0108	0.997	0.96	1.08	+/- 0.29	K	1.08	2.086
Ca-K	0.5527	1.030	49.30	56.95	+/- 1.44	Ca	56.95	107.238
Mg-K	0.0095	1.324	1.80	1.26	+/- 0.18	Mg	1.26	3.916
O -K	---	4.264	11.03	5.09 S	---	---	---	---
Total			100.00	100.00			100.00	193.518

Figure 4. SEM and XRD analysis of chloride diffused samples (Transition zone).

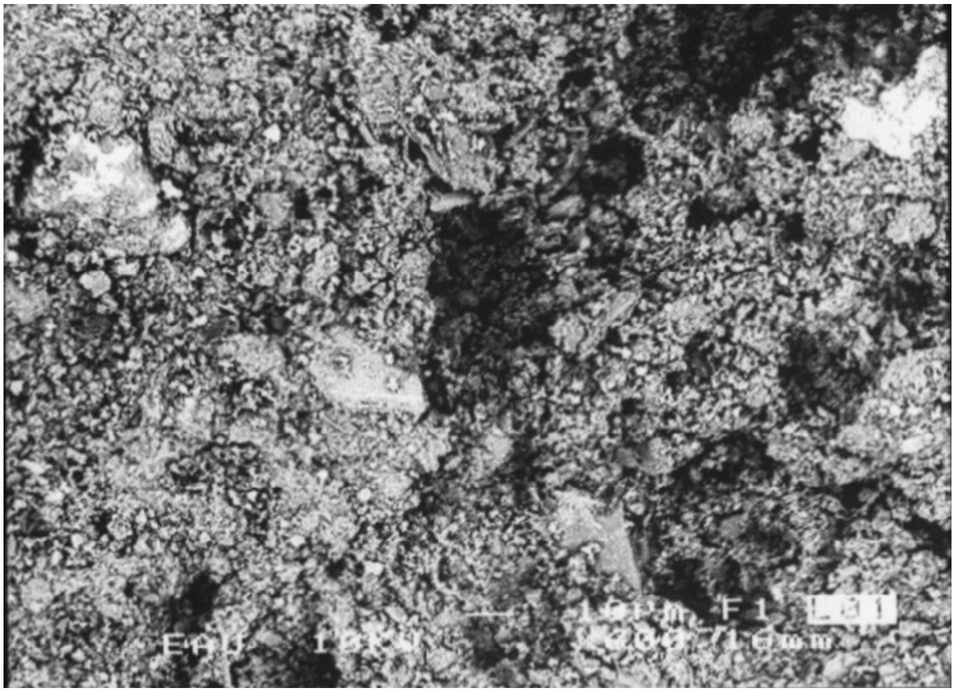

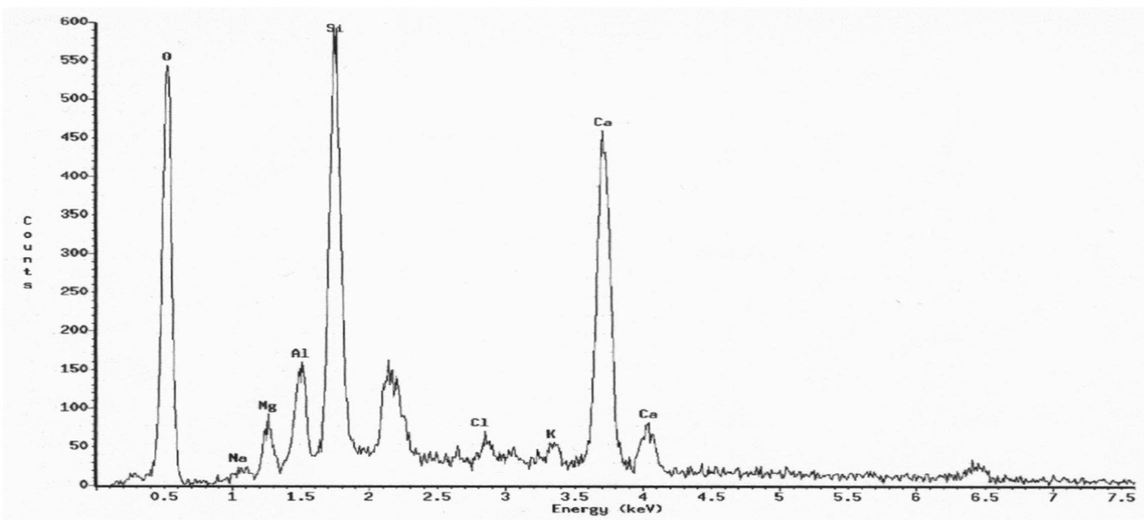

PROZA Correction Acc.Volt.= 10 kV Take-off Angle=30.98 deg
Number of Iterations = 4

Element	k-ratio (calc.)	ZAF	Atom %	Element Wt %	Wt % Err. (1-Sigma)	Compound Formula	Compound Wt %	No. of Cations
Fe-K	0.1063	1.168	7.54	12.42	+/- 2.64	Fe2O3	17.75	16.000
Cl-K	0.0049	1.098	0.52	0.54	+/- 0.23	Cl	0.54	1.097
Ag-L	0.0000	1.286	0.00	0.00	+/- 0.00	Ag2O	0.00	0.000
Si-K	0.1949	1.125	26.47	21.93	+/- 0.49	Si	21.93	56.178
Al-K	0.0435	1.218	6.65	5.30	+/- 0.36	Al	5.30	14.124
K -K	0.0170	1.016	1.50	1.73	+/- 0.30	K	1.73	3.186
Ca-K	0.4841	1.038	42.51	50.25	+/- 1.29	Ca	50.25	90.217
Mg-K	0.0190	1.320	3.50	2.51	+/- 0.18	Mg	2.51	7.428
O -K	---	4.128	11.31	5.34 S	---	---	---	---
Total			100.00	100.00			100.00	188.230

Figure 5. SEM and XRD analysis of chloride diffused sample (White sediment observed section).

Table 5. Compressive strength, total load, penetration depth, and chloride contents of the mixtures.

	UCS (kg/cm^2)		ETL (C)		ETP (mm)		Volhard* (kg/m^3)	
	WC	AC	WC	AC	WC	AC	WC	AC
0M013500♣	447.22	346.29	3029.191	3560.5809	8.74	18.29	2.96	5.88
0M014000	317.35	255.99	4004.465	4761.3757	40.00	45.99	10.66	15.20
0M014400	255.38	212.01	4469.433	5240.8159	44.00	47.46	11.36	21.95
0M015000	203.63	186.48	4777.448	5494.0502	44.99	47.95	17.44	25.87
20M023500	380.50	339.46	3906.304	4626.6508	13.10	14.15	4.36	4.83
20M024000	278.88	217.01	5679.5459	7214.7409	22.38	32.98	6.70	8.63
20M024400	231.75	184.79	7655.2631	8702.4037	42.00	46.97	10.41	18.41
20M025000	187.96	167.04	8957.9345	10976.293	47.94	48.43	20.34	39.21
30M033500	385.81	303.65	5092.4644	6079.8619	15.71	16.75	4.97	5.55
30M034000	266.57	212.75	5584.9671	6485.4130	15.19	17.78	5.31	5.77
30M034400	229.88	187.40	6373.6823	7389.2609	17.27	19.32	5.70	6.09
30M035000	198.53	167.75	8187.1727	9602.5900	20.34	22.38	6.26	6.79
0M543500	455.68	351.81	912.4520	1065.8691	6.40	9.31	1.64	2.97
0M544000	397.75	287.45	1263.1950	1458.1076	11.50	11.50	3.77	3.77
0M544400	328.29	270.34	1461.9340	1785.4499	10.96	9.30	3.82	2.87
0M545000	286.53	222.32	1044.8490	1229.0299	9.30	12.03	3.12	3.94
0M053535	535.22	399.34	1642.5010	1955.1269	9.86	13.62	3.20	4.57
0M054035	389.81	315.76	2167.7000	2684.8325	19.32	25.42	6.11	7.27
0M054435	356.90	279.16	2669.5420	3117.4378	24.91	26.93	7.02	7.60
0M055035	356.21	300.64	3325.8730	3916.5191	27.44	27.44	7.61	7.64
0M063550	474.38	410.75	1252.4590	1579.4502	7.59	10.95	2.40	3.52
0M064050	371.08	290.65	1848.0950	2206.0463	14.67	22.88	5.02	6.90
0M064450	352.99	262.71	2139.4630	2645.2696	21.87	32.98	7.07	8.60
0M065050	310.00	252.39	2819.3370	3159.2542	35.99	41.50	9.27	11.03
0M573535	473.09	434.64	1437.7550	1675.4663	9.30	12.03	2.76	4.11
0M574035	399.28	315.20	1898.1849	2105.0613	13.62	22.38	5.14	6.76
0M574435	328.89	253.61	2208.5090	2641.9826	20.34	32.47	6.29	8.53
0M575035	219.30	180.02	2727.9151	3210.9353	33.98	40.50	8.88	10.54
25M583500	404.69	310.71	2603.5597	2959.9269	14.15	17.27	5.01	5.66
25M584000	328.22	256.32	2760.1012	3366.8859	15.71	20.85	5.41	6.43
25M584400	251.97	204.21	2961.1850	3708.1641	18.29	22.88	5.94	6.88
25M585000	202.17	170.11	3684.4670	4279.8478	23.39	31.47	6.74	8.35

WC: Water cured; AC: Air cured; UCS: Compressive strength according to ultrasonic pulse velocity; ETL: Electrochemical total load; ETP: Electrochemical total penetration depth. *Chloride content of the concrete at 7 mm according to Volhard method.

RESULTS AND DISCUSSION

Chloride ingress in cementitious systems is a complicated phenomenon. The chloride ingress is lower around aggregates than other parts of concrete samples. The cement paste and the interface properties of the chloride durable concrete have to be well qualified. The additives like SF, FA and GBFS, which delays the hydration, have positive effects on the chloride permeability of concrete. A well defined and completed curing process, results in lower permeability and the additives also enhances the impermeability. Specifically, the deficient curing of concrete enhances the permeability. Thus, the durability of this kind of concrete may be a problem.

According to the observed chloride permeability tests for silica fume added to concrete, the chloride resistivity of concrete is enhanced four times than the no additive concrete. However, GBFS did not enhance the chloride resistivity as the silica fumes are added concrete, but the enhancement of chloride resistivity is as great as two times according to no additive concrete. The replacement of GBFS by weight of cement given as 35%, the optimum chloride resistivity values are obtained but this percentage may be increased to 50% in order to have more economic concrete. In the effect of FA added concrete mixtures, the only positive effect on chloride resistivity is observed for the concrete with 0.35 water-cement ratio (Table 5).

One of the other factors effecting chloride resistivity is the curing process. The whole water cured specimens had a better chloride resistivity than air cured specimens, as expected. When the water-cement ratio variation is examined with the chloride resistivity, strength and fresh unit weight test results, only the fresh unit weight was increased, while the others were decreased (Table 5).

When the additive content of concrete is known, the chloride resistivity of concrete may be obtained within the approximation of 95% according to obtained empiric formulations given as:

$$Q_h = (c_1 x Q_s + c_2) \quad (1)$$

where Q_h is total load for air cured sample (C), Q_s is total load for water cured sample (C), c_1 and c_2 are the coefficients given as c_1 = 1.19201657 and c_2= -14.1818516 for the effect of air and water cure to total load (R^2 = 0.99):

$$v_h=(c_1 x v_s + c_2) \quad (2)$$

where V_h is total chloride penetration depth for air cured sample (mm), Q_s is total chloride penetration depth for water cured sample, c_1 and c_2 are coefficients Given as c_1 = 1.02809575 and c_2 = 3.9165194 for the effect of air and water cure to total load (R^2 = 0.95):

1. Mix

$$Cl_m = (0.000178) \times (Q^{(-2.312952)} + (0.000000037720) \times Q^{(3.357182)} + (-163.839)) \quad (3)$$

2. Mix

$$Cl = (0.006393) \times (Q^{(-3.5466355)} + (1.85739E-15) \times Q^{(4.5849703)} + (638.591)) \quad (4)$$

3. Mix

$$Cl_m = (73.5589) \times (Q^{(0.0280368)} + (-863.117) \times Q^{(-20.426145)} + (-1.2016)) \quad (5)$$

4. Mix

$$Cl_m = (720.277) \times (Q^{(-0.0216929)} + (-7367.86) \times Q^{(-1.880275)} + (-0.8401)) \quad (6)$$

5. Mix

$$Cl_m = (266.486) \times (Q^{(-0.0632326)} + (-717.762) \times Q^{(-1.235605)} + (-0.53816)) \quad (7)$$

6. Mix

$$Cl_m = (1010.879) \times (Q^{(0.0088736)} + (-24722.9) \times Q^{(-1352.7295)} + (-1.063552)) \quad (8)$$

7. Mix

$$Cl_m = (1581.23) \times (Q^{(-641.08813)} + (0.75442) \times Q^{(0.0079398)} + (-0.797746)) \quad (9)$$

8. Mix

$$Cl_m = (0.001210) \times (Q^{(0.2332569)} + (1.5963) \times Q^{(1.0011534)} + (-36.2899)) \quad (10)$$

where Cl_m is total chloride content (kg/m^3), Q is total load (C) (R^2=0.95), for the related concrete mix groups.

$$v_r = (c_1 x v_v) \quad (11)$$

where V_r is total chloride penetration depth obtained from Color Analysis Method (mm), V_v is total chloride penetration depth obtained from Volhard Method (mm), c_1 is a coefficient given as c_1 = 1.013575 for the comparison of chloride penetration depth for Color Analysis Method and Volhard Method (R^2 = 0.99). Despite all mentioned experimental techniques, the Color Analysis Method performs approximately the same estimation without any complexity with the Equation given as:

$$Cl_m = (c_1) \times (v^{(c2)} + (c_3)) \times LOG10(v) + c_4 \times EXP(v x c_5) \quad (12)$$

where v is total chloride penetration depth (mm), c_1, c_2, c_3, c_4, and c_5, are the coefficients given as c_1 = 135.796703, c_2 = 0.0153816534, c_3 = -1.01207214, c_4 = 0.000000000133799863, and c_5 = 0.527549306, for the chloride penetration depth according to chloride content (R^2 = 0.98).

The effect of additive content on the conductivity of concrete resulted in more variation in chloride resistivity, due to the conductivities of different additives.

White sediment is observed above the surfaces of the chloride diffused, and $AgNO_3$ sprayed concrete samples, due to $Cl + AgNO_3 \rightarrow AgCl + NO_3$ reaction. The white sediment, which is observed as a result of Cl^- ions, is AgCl and verified by SEM analysis (Figures 3, 4, and 5). When this white sediment (AgCl) is exposed to sun rise, its color transforms to purple and then to black. This type of color transformation results in errors, while observing the color transformation gap. Thus, for the color analysis, the $AgNO_3$ sprayed concrete samples have to be digitized as soon as possible. The variation of chloride content and chloride penetration depth is directly proportional (above 98%) with the depth of color transforming pixels (Figures 6 and 7).

Conclusion

A fast, reliable method to determine the chloride concentration in cement-based materials can save significant time and money. Engineers and researchers responsible for testing and monitoring cement-based materials for corrosion performance can economically determine the chloride concentration of a larger number of samples in a relatively shorter time if correlations between the faster and slower methods can be

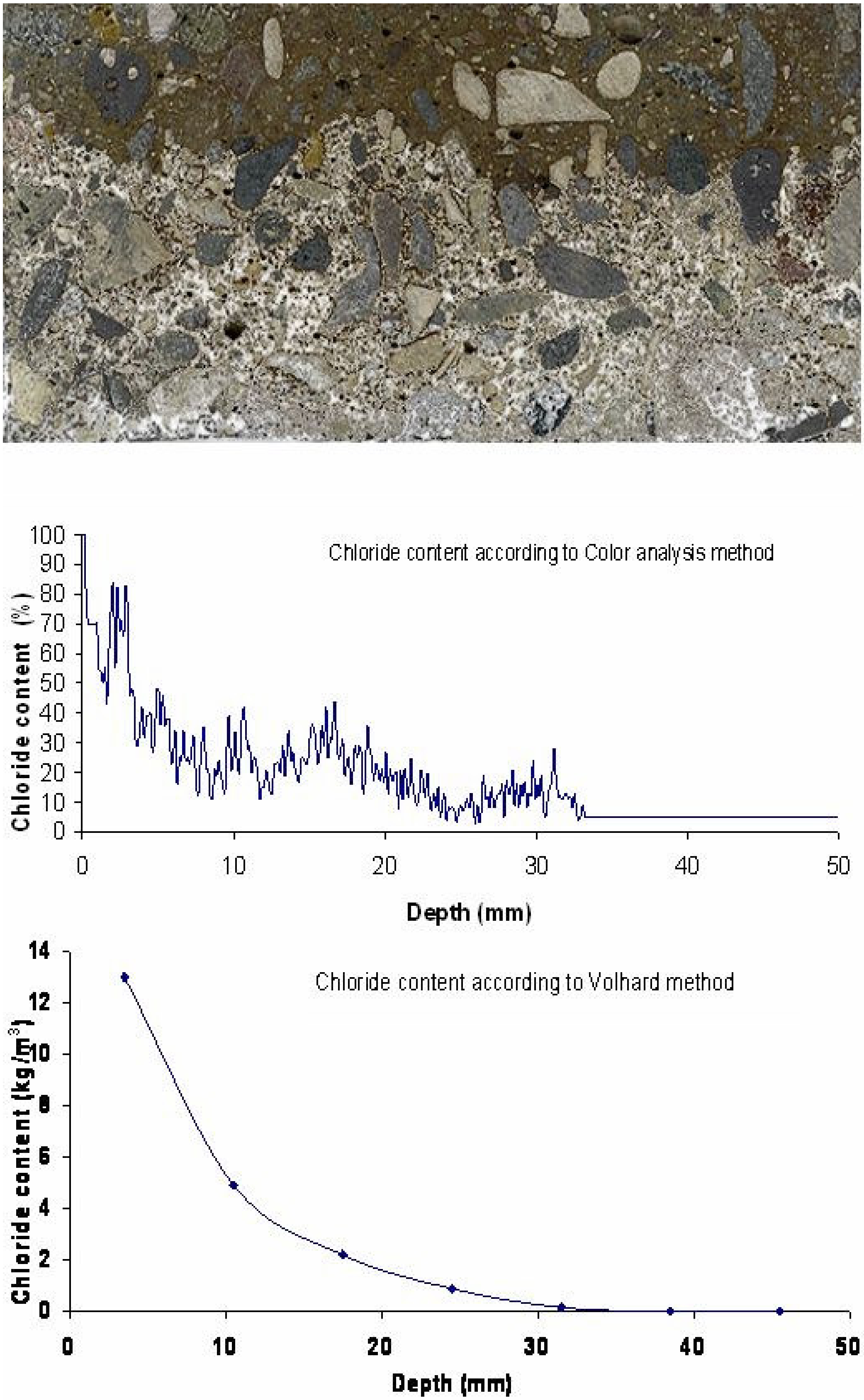

Figure 6. Chloride penetration depth according to Volhard and Color analysis method (air cured).

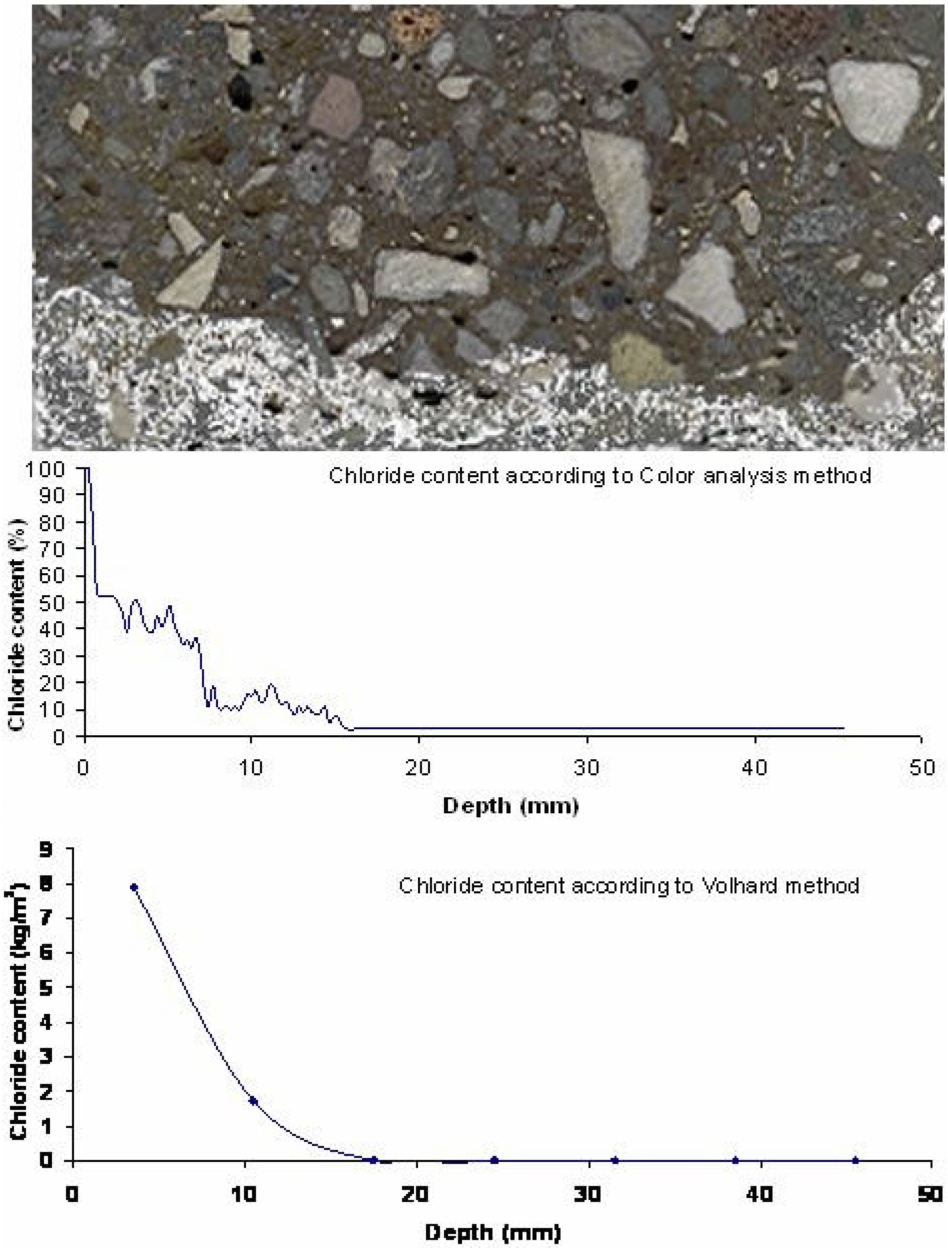

Figure 7. Chloride penetration depth according to Volhard and Color analysis method (water cured).

determined. The results obtained from this study indicate that the measurements obtained from the Color Analysis Method and the tested, other method samples are highly correlated. Results from this research clearly indicate that the Color Analysis method for assessing the chloride penetration depth is applicable to various cement-based systems. Future research should examine and modify the calibration procedure of the method, to take into account, the ions coming from unconventional aggregates, as suggested in the literature, to decrease the difference between the results of the variable methods.

REFERENCES

ACI 201.2R–01 (2001). Guide to Durable Concrete," ACI Committee 201 on Durability of Concrete, American Concrete Institute, Farmington Hills, Michigan, USA.

Asociacion Espanola de Normalizacion y Certificacion (1991). Norma UNE 80-217-91, 'Determination of chloride ions in cement by the Volhard's method', Madrid, Spain.

Asociacion Espanola de Normalizacion y Certificacion (1994). Norma UNE 112-010-94, 'Determination of chloride ions in concrete', Madrid, Spain, (in Spanish).

Aydın AC (2007). Self Compactability of High Volume Hybrid Fiber Reinforced Concrete, Construction and Building Materials, 21: 1146-1151.

Aydın AC, Arslan A, Gül R (2007). Mesoscale Simulation of Cement Based Materials' Time Dependent Behavior , Comput. Mat. Sci., 41/1: 20-26.
Aydın AC, Düzgün OA, Tortum A (2008). Determination of the Optimum Conditions for Steel Fibers on the Mechanical Properties of Natural Lightweight Aggregate Concrete, Pollack Perodika, 3(1): 101-112. (SCI değil)
Aydın AC, Gül R (2007). Influence of Volcanic Originated Natural Materials as Additives on the Setting Time and Some Mechanical Properties of Concrete, Construction and Building Materials, 21: 1274-1278.
Aydın AC, Karakoç MB, Düzgün OA, Bayraktutan MS (2010). Effect of low quality aggregates on the mechanical properties of lightweight concrete, Sci. Res. Essays, 5 (10): 1133-1140.
Aydın AC, Tortum A, Yavuz M (2006). Prediction of concrete elastic modulus using adaptive neuro-fuzzy inference system, Civil Eng. Environ. Sys., 23: 295-309.
Basset J, Denney RC, Jeffery GH, Mendham J (1978). Vogel's Textbook of Quantitative Inorganic Analysis', Longman, London.
Chau KW (2002). Field measurements of SOD and sediment nutrient fluxes in a land-locked embayment in Hong Kong, Adv. Environ. Res., 6(2): 135-142.
Chau KW (2000). Transverse mixing coefficient measurements in an open rectangular channel," Adv. Environ. Res., 4(4): 287-294.
Chau KW (2004). Investigation on effects of aggregate structure in water and wastewater treatment," Water Sci. Technol., 50(12): 119-124.
Düzgün OA, Gül R, Aydın AC (2005). Effect of steel fibers on the mechanical properties of natural lightweight aggregate concrete, Mater. Lett., 59: 3357-3363.
Erdoğdu Ş, Kondratova IL, Bremner TW (2004). Determination of chloride diffusion coefficient of concrete using ope-circuit potentials, Cement Concrete Res., 34: 603-609.
Goodspeed CH, Vanikar S, Cook RA (1996). High Performance Concrete Defined for Highway Structures. ACI Concrete Int., 18(2): 62-67.
Gül R, Okuyucu E, Türkmen I, Aydın AC (2007). Thermo-mechanıcal propertıes of fiber reinforced raw perlıte concrete, Mater. Lett., 61/29, 5145-5149.
Güneyisi E, Özturan T, Gesoğlu M (2007). Effect of Initial Curing on Chloride Ingress and Corrosion Resistance Characteristics of Concretes Made with Plain and Blended Cements", Building and Environment, 42(7): 2676-2685.
Halmen C, Trejo D (2007). Measuring chloride concentrations for various cement-based systems, ACI Mater. J. 104(6): 567-574.
Hasar UC, Akkaya G, Aktan M, Gozu C, Aydın AC (2009). Water-To-Cement Ratio Prediction Using ANNs From Non-Destructive And Contactless Microwave Measurements, Progress In Electromagnetics Research, PIER 94: 311-325.
Hasar UC, Simsek O, Aydın AC (2010). Application of Varying-Frequency Amplitude-Only Technique for Electrical Characterization of Hardened Cement-Based Materials, Microwave Optical Technol. Lett., 52 (4): 801-805.
Jaegermann C (1990). Effect of Water-Cement Ratio and Curing on Chloride Penetration into Concrete Exposed to Mediterranean Sea Climate, ACI Mater. J., 87(4): 333-339.
Jin Z, Sun W, Zhang YS, Jiang JY, Lai JZ (2007). Interaction between sulfate and chloride solution attack of concretes with and without fly ash. Cement Concr. Res. 37: 1223-1232.
Marinus ATMB (2002). The alkali-silica reaction: mineralogical and geochemical aspects of some Dutch concretes and Norwegian mylonites, Thesis. - Proefschrift Universiteit Utrecht.
Meck E, Sirivivatnanon V (2003). Field indicator of chloride penetration depth, Cement Concrete Res., 33(8): 1113-1117.
Nagesh M, Bhattacharjee B (1998). Modeling of Chloride Diffusion in Concrete and Determination of Diffusion Coefficients, ACI Mater. J., 95(2): 113-120.
Oğuz E, Aydın AC (2003). Prediction Of Adsorption Velocity Of Phosphate Removal From Wastewater With Gas Concrete, Including Ph, Temperature, And Agitation Speed, Int. J. Environ. Poll., 19: 603-614.
Ozyildirim C, Halstead W (1988). Resistance to Chloride Ion Penetration of Concretes Containing Fly Ash, Silica Fume, or Slag, Permeability of Concrete, SP-108, American Concrete Institute, Farmington Hills, MI, pp. 35-61.
Page CL, Page MM (2007). Durability of Concrete and Cement Composites, Woodhead Publishing, Cambridge, 416: (ISBN 978-1-85573-940-6).
RILEM TC 178-TMC (2002). Recommendation for analysis of total chloride in concrete. Mat. Struct. 35: 583-585.
Saito M, Ishimori H (1995). Chloride Permeability of Concrete Under Static and Repeated Compressive Loading. Cement Concrete Res., 25(4): 803-808.
Samaha HR, Hover KC (1992). Influence of Microcracking on the Mass Transport Properties of Concrete. ACI Materials J., 89(4): 416-424.
Song HW, Lee CH, Ann KY (2008). Factors influencing chloride transport in concrete structures exposed to marine environments, Cem. Concr. Com. 30(2): 113-121.
Titherington MP (1998). The influence of steam curing on chloride resistance of high performance concrete, M.A.Sc Thesis, University of Toronto.
Topcu IB, Boga AR, Hocaoglu FO (2009). Modeling corrosion currents of reinforced concrete using ANN, Automation in Construction, 18(2): 145-152.
Tortum A, Celik C, Aydın AC (2005). Determination of the Optimum Conditions for Tire Rubber In Asphalt Concrete, Building Environ., 40: 1492-1504.
Türkmen I, Gül R, Çelik C, Demirboğa R (2003). Determination by the Taguchi method of optimum conditions for mechanical properties of high strength concrete with admixtures of silica fume and blast furnace slag, Civil Eng. Environ. Syst., 20(2): 105-118.